

# Parameter optimization of tuned inerter-negative-stiffness damper for wind-excited high-rise buildings

Weiwei Zhao<sup>1</sup>, Yong Quan<sup>1</sup>

<sup>1</sup>*State Key Laboratory of Disaster Reduction in Civil Engineering, Tongji University, Shanghai 200092, China. weiwei\_zero@tongji.edu.cn.*

## SUMMARY:

Inerter can reduce the mass and volume of the damper while ensuring the control effect, and negative stiffness devices can make the frequency band controlled by the damper wider. But when two devices work together, the optimal control theory is more complex. Most of the existing research objectives are single degree-of-freedom structures under harmonic or seismic excitations. This study derives a numerical method for calculating the optimal damping ratio and frequency ratio of tuned inerter-negative-stiffness damper (TINSD) installed on a two degree-of-freedom model based on  $H_2$  optimization. And the optimization is used to control the wind-induced response of the multi-degree-of-freedom system. The results show that the control effect of TINSD is obviously better than that of traditional tuned inerter damper in the controlling of wind-induced vibration of the structure. And the optimal parameters of TINSD calculated based on the generalized two degree-of-freedom model are still applicable to the multi degree-of-freedom.

*Keywords: Tuned inerter-negative-stiffness,  $H_2$  optimization, wind-induced vibration*

## 1. INTRODUCTION

In order to solve the problem of excessive mass of traditional dynamic vibration absorber (DVA) (Frahm, 1909) when controlling wind vibration response of super high-rise buildings, Lazar et al. (2014) introduced inerter into DVA and proposed TID. In order to further improve the vibration control performance of DVA, the negative stiffness device (NSD) (Lakes, 2001) with high static-low dynamic stiffness was introduced into vibration control. Shen et al. (2017) first explored several negative stiffness DVAs and optimized their parameters. Wang et al. (2019) optimized the parameters of four kinds of inerter-based dynamic vibration absorbers with negative stiffness (INDVAs) and evaluated the performance of INDVAs compared with existing DVAs under harmonic and random excitation.

Most of the existing research is based on SDOF systems under harmonic or seismic excitation, and here are few researches on the multi-degree-of-freedom (MDOF) structure under wind load. Moreover, the calculation method of the optimal parameters of INDVAs installed on the MDOF structure is quite complicated.

In this study, a tuned inerter-negative-stiffness damper (TINSD), as a kind of INDVA, is studied. TINSD installed on a generalized 2DOF model is firstly optimized based on  $H_2$  optimization, and then the optimized TINSD is applied to a high-rise buildings under wind load excitation.

## 2. DYNAMIC MODEL AND H<sub>2</sub> OPTIMIZATION OF TINS D

Because TINS D is a two-terminal device, the optimization objective in this section is a 2DOF model with TINS D installed for simplifying the derivation.

### 2.1. Governing equation of the 2DOF-TINS D system

Figure 1 shows the 2DOF-TINS D system. The negative stiffness is paralleled with the inerter in TID. TINS D consists of a spring having positive stiffness coefficient  $k_d$  (N/m), a spring having negative stiffness coefficient  $k_N$  (N/m), a dashpot element having coefficient  $c_d$  (N·s/m), and an ideal inerter having inertance  $b$  (kg).

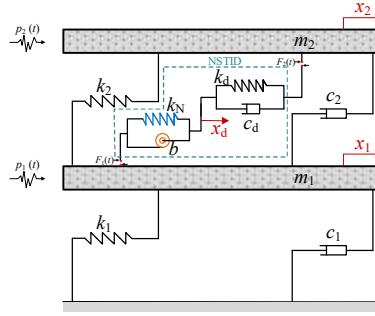


Figure 1. Lumped mass model of an 2DOF system under TINS D control.

Following the D'Alembert principle, the equations of motion of the 2DOF-TINS D system is expressed as

$$\mathbf{M}\ddot{\mathbf{x}}(t) + \mathbf{C}\dot{\mathbf{x}}(t) + \mathbf{K}\mathbf{x}(t) = \mathbf{P}(t) + \mathbf{F}(t) \quad (1)$$

where  $\mathbf{M}$ ,  $\mathbf{C}$ , and  $\mathbf{K}$  are the mass, damping, and stiffness matrices of the uncontrolled MDOF structure, respectively.  $\mathbf{x}(t)$ ,  $\dot{\mathbf{x}}(t)$ ,  $\ddot{\mathbf{x}}(t)$ , and  $\mathbf{P}(t)$  are the displacement, velocity, acceleration, and excitation force vectors, respectively.  $\mathbf{F}(t) = \{F_1(t), -F_2(t)\}$ ,  $F_1(t)$  and  $F_2(t)$  are the control forces of TINS D exerted on the first and the second layers of the structure, respectively.  $x_d(t)$ ,  $x_1(t)$ , and  $x_2(t)$  are the displacement of the attached mass, the first and the second DOF, respectively.  $k_d$ ,  $k_N$ , and  $c_d$  are the positive stiffness, negative stiffness and damping of TINS D, respectively.  $b$  is the inertance in kg. The physical mass of TINS D is  $m_d$ , which can be negligible compared to  $b$ .

To make it easier to be dimensionless, it's assume that  $m_1 = m_2$ ,  $c_1 = c_2$ ,  $k_1 = k_2$ . Eq. (1) can be expressed in the frequency domain as

$$\mathbf{R}(\omega)\mathbf{x}(\omega) = \mathbf{M}^{-1}\mathbf{P}(\omega) \quad (2)$$

$$R_{1,1}(\omega) = (-\omega^2 + 4i\omega\omega_s\zeta_s + 2\omega_s^2 - \omega^2\beta - \mu\nu_N^2\omega_s^2) + A_1(\omega)(\omega^2\beta - \mu\nu_N^2\omega_s^2) \quad (3)$$

$$R_{1,2}(\omega) = (-2i\omega\omega_s\zeta_s - \omega_s^2) + A_2(\omega)(\omega^2\beta - \mu\nu_N^2\omega_s^2) \quad (4)$$

$$R_{2,1}(\omega) = (-2i\omega\omega_s\zeta_s - \omega_s^2) + A_1(\omega)(2i\mu\omega\omega_d\zeta_d - \mu\nu_d^2\omega_s^2) \quad (5)$$

$$R_{2,2}(\omega) = (-\omega^2 + 2i\omega\omega_s\zeta_s + \omega_s^2 + 2i\mu\omega\omega_d\zeta_d + \mu\nu_N^2\omega_s^2) + A_2(\omega)(2i\mu\omega\omega_d\zeta_d - \mu\nu_N^2\omega_s^2) \quad (6)$$

where  $A_1(\omega) = \frac{-\omega^2\beta + \nu_N\omega_s^2}{-\omega^2\beta + 2i\mu\omega\omega_d\zeta_d + \nu_d\omega_s^2 + \nu_N\omega_s^2}$ ,  $A_2(\omega) = \frac{2i\mu\omega\omega_d\zeta_d + \nu_d\omega_s^2}{-\omega^2\beta + 2i\mu\omega\omega_d\zeta_d + \nu_d\omega_s^2 + \nu_N\omega_s^2}$ .  $\omega_s = \sqrt{k_1/m_1}$ ,  $\omega_d = \sqrt{k_d/m_d}$ , and  $\omega_N = -\sqrt{-k_N/m_d}$  are natural frequency of structure, positive and negative

frequency of TINS D.  $\zeta_s = c_1/(2m_1\omega_s)$  and  $\zeta_d = c_d/(2m_d\omega_d)$  are damping ratios of structure and TINS D.  $\nu_d = \omega_d/\omega_s$  and  $\nu_N = \omega_N/\omega_s$  are positive and negative frequency ratios.  $\mu = m_d/m_1$  and  $\beta = b/m_1$  are the actual mass ratio and the inertial mass ratio, respectively.

## 2.2. $H_2$ optimization based on Lyapunov algorithm

The objective of  $H_2$  optimization is the standard deviation (STD) of structural displacement response under white noise.  $\|x_2(\omega)\|_2^2$  is set as the optimal objective here.

$$J = \int_0^{\omega_{sup}} \left| \frac{R_{2,1}(\omega) - R_{1,1}(\omega)}{R_{2,1}(\omega)R_{1,2}(\omega) - R_{1,1}(\omega)R_{2,2}(\omega)} \right|^2 d\omega, \quad (7)$$

where  $\omega_{sup}$  is the upper bound of the integral.  $J$  can be simplified based on Lyapunov equation. In order to find the optimal  $\zeta_d$ ,  $\nu_d$ , and  $\nu_N$ , the partial differential equation needs to be satisfied:

$$\frac{\partial J}{\partial \zeta_d} = \frac{\partial J}{\partial \nu_d} = \frac{\partial J}{\partial \nu_N} = 0 \quad (8)$$

The process of directly solving Eq. (8) is very complicated, and it is difficult to get an explicit analytical solution. Therefore, it is suggested to use numerical method to calculate the optimal  $\zeta_d$ ,  $\nu_d$ , and  $\nu_N$  under the corresponding  $\mu$  and  $\beta$ .

## 3. PERFORMANCE EVALUATION OF TINS D IN A MDOF STRUCTURE UNDER WIND EXCITATIONS

Assume that the two terminals of TINS D are connected at  $a^{\text{th}}$  and  $(a-p)^{\text{th}}$  layer of the MDOF structure, respectively.

### 3.1. Building information and wind excitations

The 420 m tall building has 84 floors with a cross section of 28 m  $\times$  140 m and a total mass of 411600 t. The synchronized multi-point pressure measurement test on the rigid model of the building was conducted in TJ-2 wind tunnel at Tongji University as shown in Figure 2(a). The mode shapes of these six modes are shown in Figure 2(b). The power spectral density (PSD) of the aerodynamic forces acting on the 84th floor at the wind direction of 90° (the most unfavourable wind direction) corresponding to a return period of 50 years is shown in Figure. 2 (c).

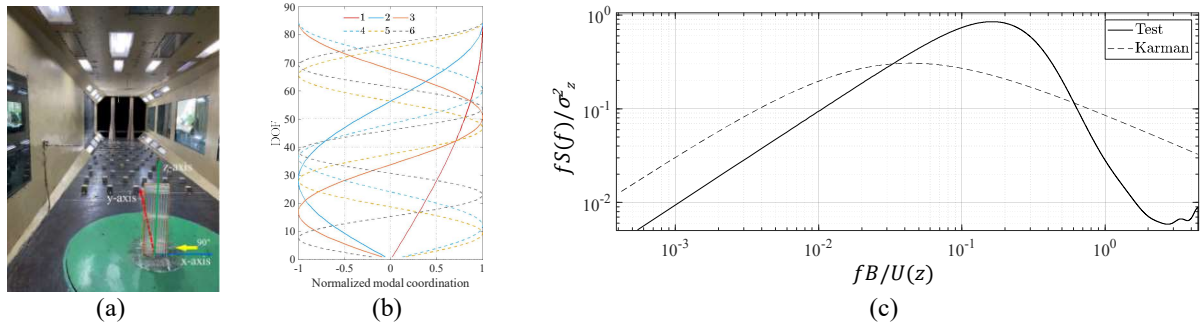


**Figure 2.** (a) Scale model in the wind tunnel test and (b) first six mode shapes. (c) PSD of the aerodynamic force on the 84th floor at the wind direction of 90°

### 3.2. Analysis of control effect

In order to keep  $\mu$  as small as possible, we set  $\mu=0.0001$  in this study. And in order to ensure the control effect of TID,  $\beta = 0.9$ . The optimal  $\zeta_d$ ,  $\nu_d$ , and  $\nu_N$  under the corresponding cases of  $\mu$  and  $\beta$  can be obtained by solving Eq. (11).  $\zeta_d = 0.46$ ,  $\nu_d = 1.19$ ,  $\nu_N = -0.26$ . And  $a=80$ ,  $p=4$ . The power spectral density (PSD) of responses on the top floor of MDOF system and standard deviations (STD) of wind-induced responses along floors controlled by TINSD and TID are shown in Figure 3.

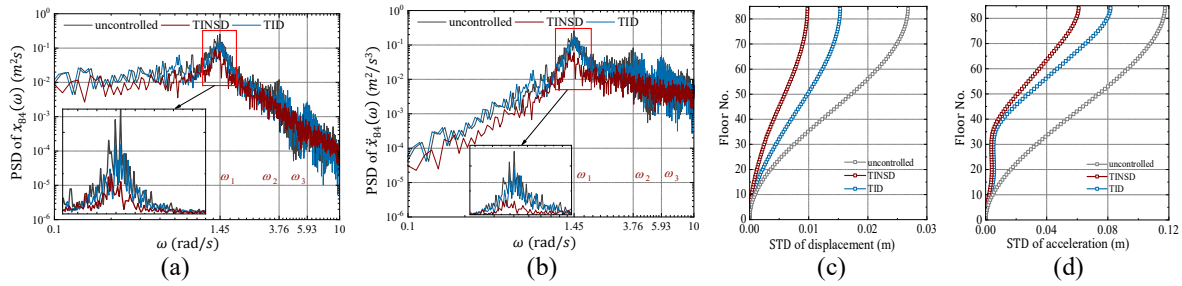


**Figure 3.** (a) displacements (b) accelerations PSDs of the top floor under the excitation acting on the top floor of the structure. (c) displacements. (d) accelerations. STDs of wind-induced responses along floors

## 4. CONCLUSIONS

This study firstly derives the analytical solution of the 2DOF structure controlled by TINSD, and a numerical method for calculating the optimal damping ratio and frequency ratio of TINSD is given based on  $H_2$  optimization. Then TINSD with optimal parameters is used to control the wind-induced response of the MDOF system. The results show that the control effect of TINSD is obviously better than that of traditional TID in the controlling of wind induced vibration of the structure. Moreover, the TINSD optimal parameters optimized by  $H_2$  based on 2DOF are still valid when applied to MDOF.

## ACKNOWLEDGEMENTS

The authors would like to acknowledge the support of the National Natural Science Foundation of China (51778493).

## REFERENCES

- Frahm H, 1909. Device for damping vibrations of bodies- US, 989958.
- Lazar IF, Neild SA, Wagg DJ, 2014. Using an inerter-based device for structural vibration suppression. *Earthquake Engineering & Structural Dynamics*, 43(8):1129-47.
- Lakes, R.S., 2001. Extreme damping in composite materials with a negative stiffness phase. *Physical Review Letters*, 86 (13): p. 2897-2900.
- Shen, Y., Peng, H., Li, X., Yang, S, 2017. Analytically optimal parameters of dynamic vibration absorber with negative stiffness. *Mechanical Systems and Signal Processing*, 85, 193-203.
- Wang X, He T, Shen Y, 2019. Shan Y, Liu X. Parameters optimization and performance evaluation for the novel inerter-based dynamic vibration absorbers with negative stiffness. *Journal of Sound and Vibration*. 463.